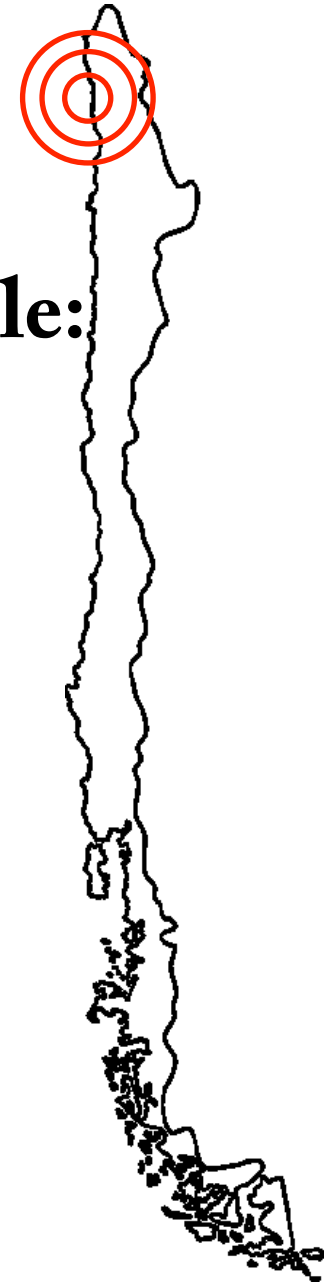




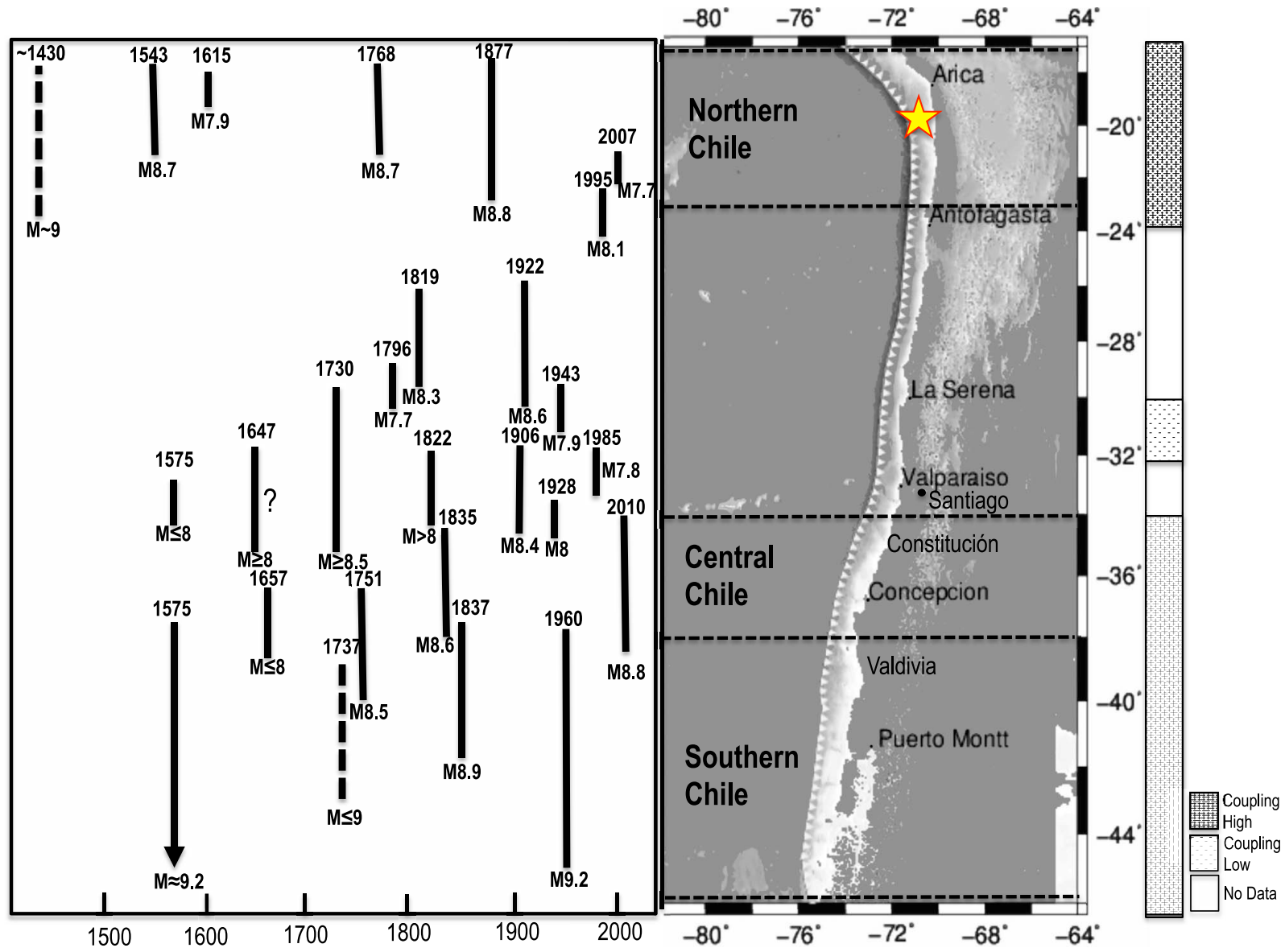
Centro de Sismologia da USP
IAG / IEE



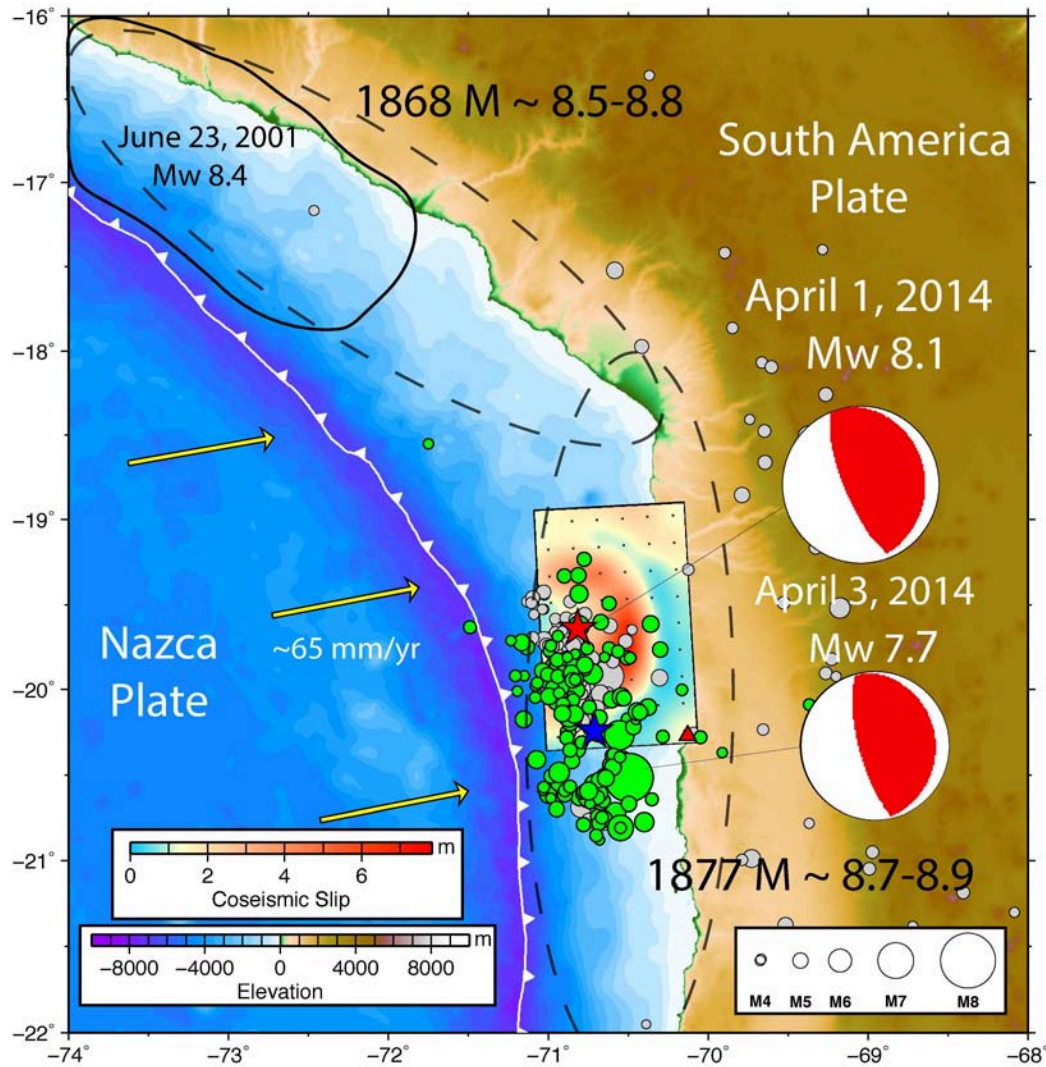
A lacuna sísmica do Norte do Chile: estado da arte

Hans Agurto-Detzel

São Paulo, 15-Setembro-2014



Scholz and Campos, 2012. *JGR*



Lay et al. (2014) GRL

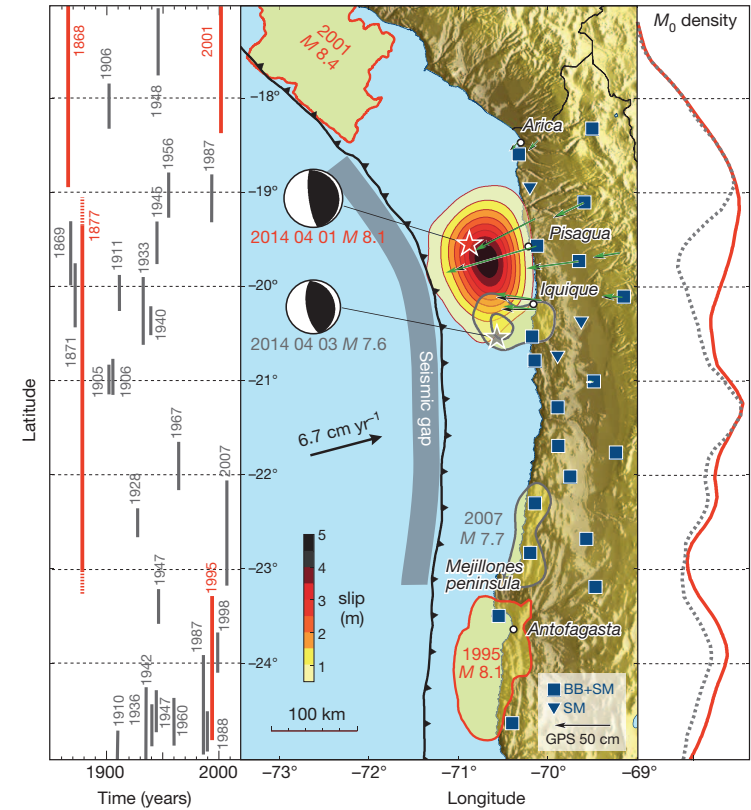


Figure 1 | Map of Northern Chile and Southern Peru showing historical earthquakes and instrumentally recorded megathrust ruptures. IPOC instruments used in the present study (BB, broadband; SM, strong motion) are shown as blue symbols. Left: historical^{1,2} and instrumental earthquake record. Centre: rupture length was calculated using the regression suggested in ref. 28, with grey lines for earthquakes $M > 7$ and red lines for $M_w > 8$. The slip distribution of the 2014 Iquique event and its largest aftershock derived in this study are colour coded, with contour intervals of 0.5 m. The green and black vectors are the observed and modelled horizontal surface displacements of the mainshock. The slip areas of the most recent other large ruptures^{4,5,7} are also plotted. Right: moment deficit per kilometre along strike left along the plate boundary after the Iquique event for moment accumulated since 1877, assuming current locking (Fig. 3a). The total accumulated moment since 1877 from 17° S to 25° S (red solid line) is 8.97; the remaining moment after subtracting all earthquake events with $M_w > 7$ (grey dotted line) is 8.91 for the entire northern Chile–southern Peru seismic gap.

Schurr et al. (2014) Nature

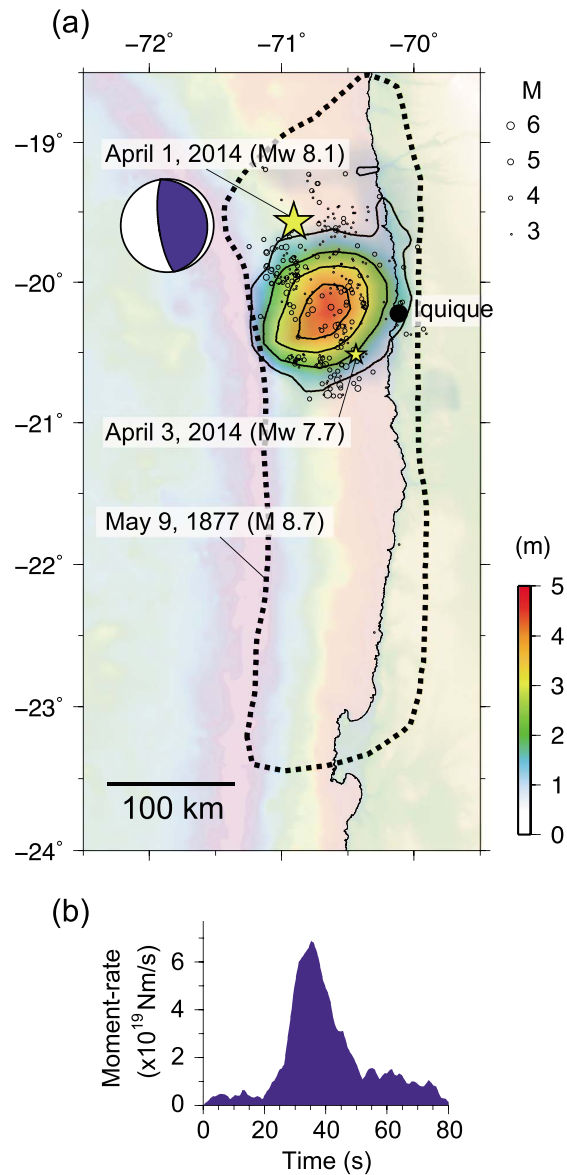


Figure 1. Total slip distribution, aftershock distribution, and moment-rate function. (a) Map view of inverted total slip distribution of the 2014 off Iquique earthquake. Large and small stars indicate the epicenter of the main shock and the largest aftershock, respectively. Also shown are the focal mechanism of main shock determined in this study and the first 2 days aftershocks (black circles), determined by the Centro Sismológico Nacional (CSN), the University of Chile. The seismic source area of 1877 off Iquique (M 8.8) earthquake [Chlieh *et al.*, 2011] is indicated by a thick dotted line. Topography and bathymetry are from ETOPO1 [Amante and Eakins, 2009]. (b) The moment-rate function of the main shock.

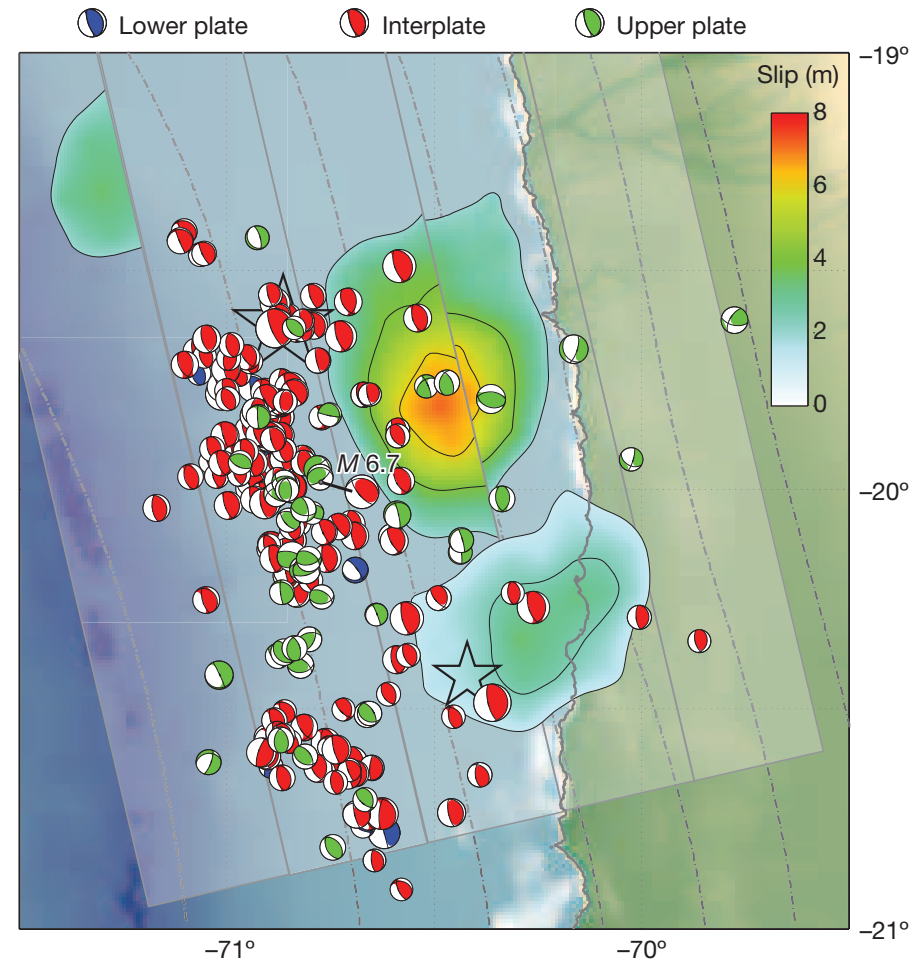


Figure 2 | Source processes of events in the March–April 2014 Iquique earthquake sequence. RMTs of relocated earthquakes in this sequence are shown and coloured by their location with respect to the slab interface; those interpreted as upper plate events are green, lower plate earthquakes are blue, and interplate events are red. Earthquakes are overlain on the preferred fault-slip models for the M 8.2 and M 7.7 events (hypocentres are shown with stars), with 2-m contour intervals. Dot-dashed lines in the background are slab contours¹³, plotted every 10 km.

Yagi *et al.* (2014) GRL

Hayes *et al.* (2014) Nature

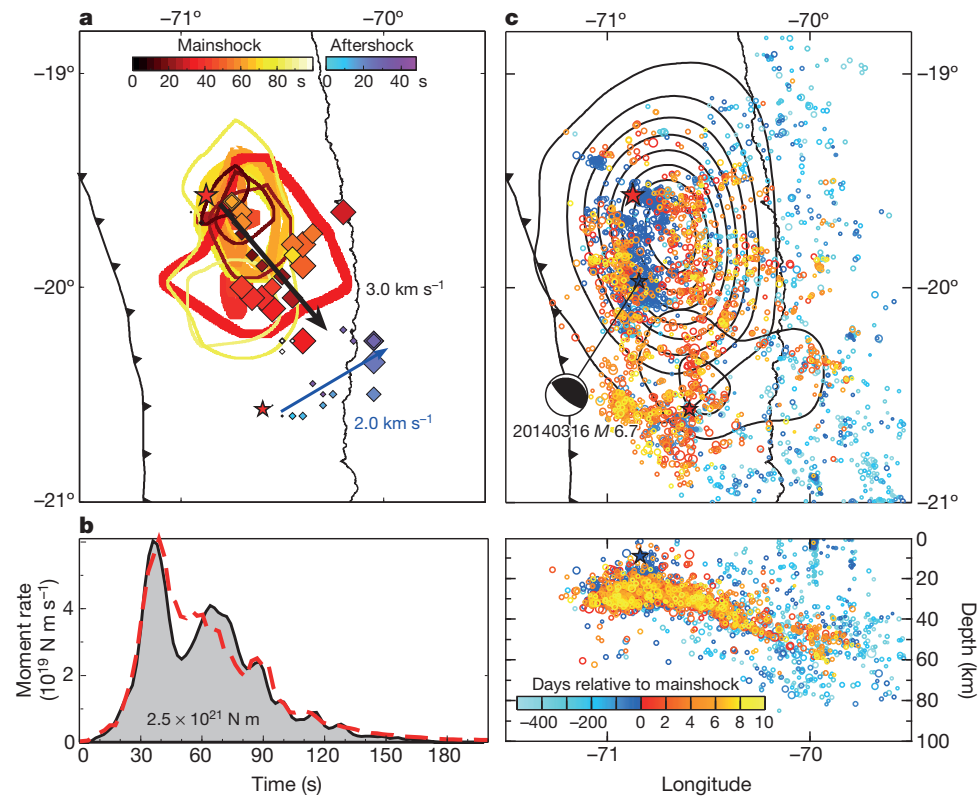


Figure 2 | Kinematic rupture development of the M_w 8.1 main and M_w 7.6 aftershock and the distribution of foreshocks and aftershocks. The nucleation point of each earthquake rupture is indicated by a coloured star. **a**, Arrows indicate the propagation of main energy release during the first 40 and 25 s for mainshock and aftershock, respectively. The contour lines represent isolines of slip rate for the mainshock from the kinematic inversion during different time intervals after rupture nucleation (0.05 m s^{-1} intervals, line thickness scaled by slip-rate). Coloured diamonds represent maxima of semblance scaled to the peak value of the emitted energy for mainshock and aftershock for each time step based on the backprojection of teleseismic

waveforms. **b**, Moment rate and time history of backprojected energy (arbitrary absolute scale). Black solid line, mainshock kinematic source-time-function; red dashed line, rescaled backprojection energy. **c**, Map (top) and longitudinal cross-section (bottom) of $\sim 3,600$ foreshocks and $\sim 1,400$ aftershocks coloured according to their time of occurrence relative to the mainshock. The slips of the mainshock and largest aftershock are contoured. The beachball depicts the double-couple of the largest M_w 6.7 foreshock that had a rupture geometry distinctively different from the mainshock and largest aftershock (Fig. 1) and a centroid depth of only 9 km (blue star) and that thus probably occurred in the upper plate.

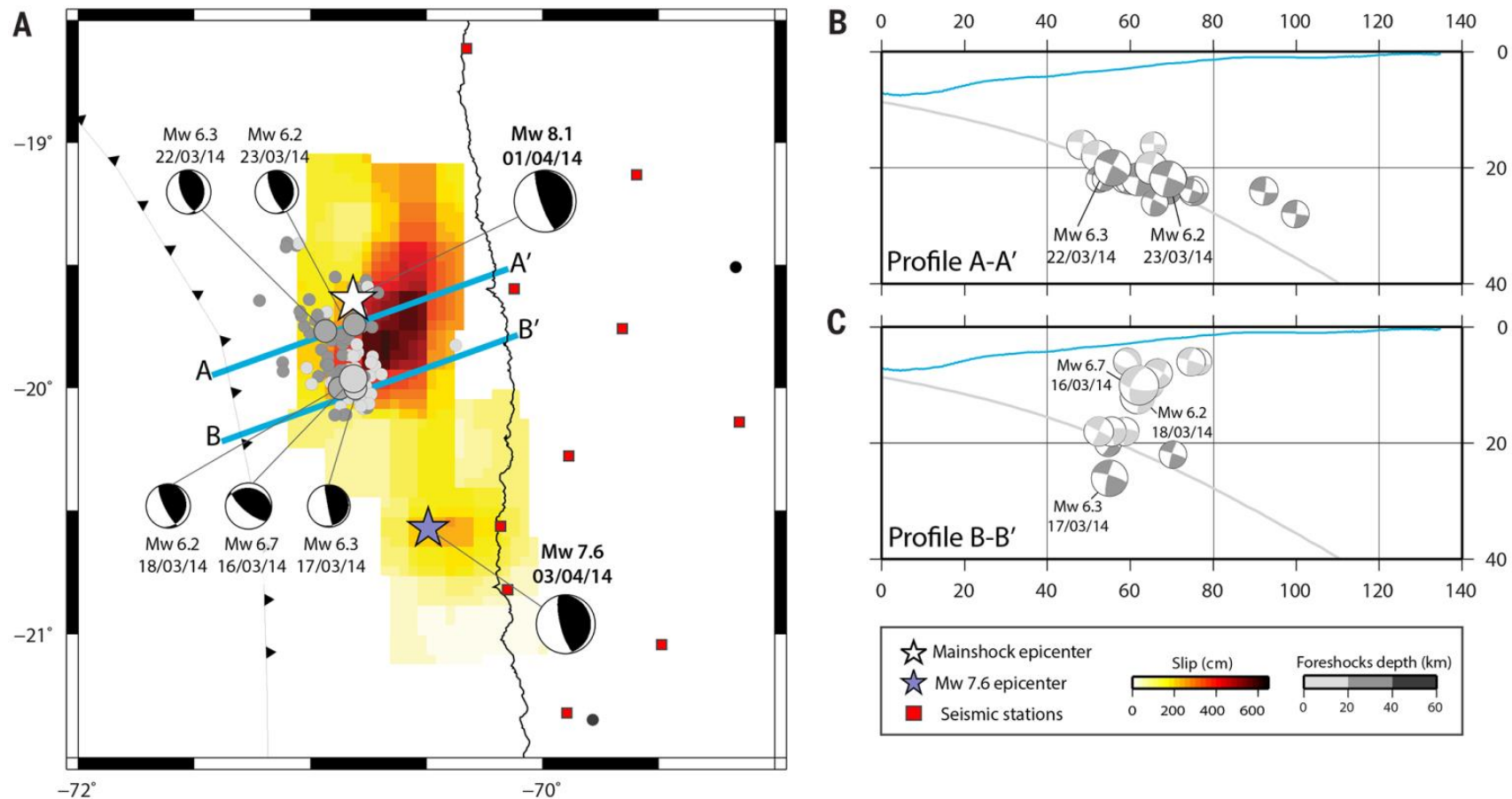


Fig. 2. Seismicity preceding the Iquique earthquake. (A) Gray dots show the foreshocks from 16 to 31 March; the intensity of gray indicates the depths of the events. The slip distribution of Mw 8.1 and Mw 7.6 earthquakes inverted from far-field broadband records of the FDSN network is shown with the color. (B) 15 km wide cross-section along the line A- A' shown in (A). (C) 15 km wide cross section along the B-B' line. In the vertical cross-sections we plot the focal mechanisms of events with Mw larger than 4.6. Mechanisms were computed by broad band moment tensor analysis. The gray curve shows the seismogenic contact according to (16).

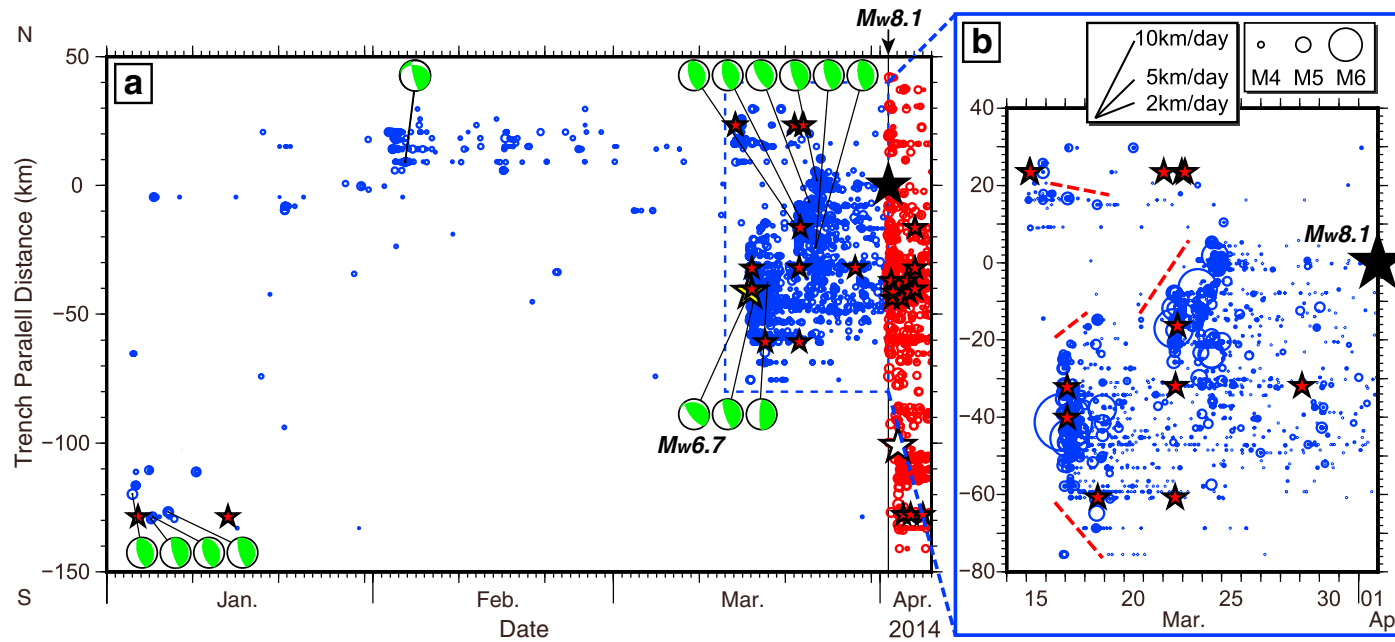


Figure 4. (a) Space-time diagram of all the detected events before and after the 2014 Iquique, Chile M_w 8.1 earthquake. The blue and red circles denote the foreshocks and aftershocks, respectively. The red stars indicate the repeating earthquakes. The diagram shows the earthquake origin times and locations projected onto the strike of the fault plane. The black, yellow, and white stars denote the hypocenters of the M_w 8.1 main shock, the largest M_w 6.7 foreshock, and the largest aftershock M_w 7.7, respectively. Focal mechanisms (from the USGS) are plotted as green beach balls. While all available focal mechanisms are used from January to February, only focal mechanisms with $M_w > 5.0$ are selected from 1 March until the main shock origin. (b) Enlargement of Figure 4a showing the intensive foreshocks between 14 March and 1 April 2014 (blue circles scaled to magnitude). The red dashed lines represent the approximate locations of the fronts of earthquake migrations.

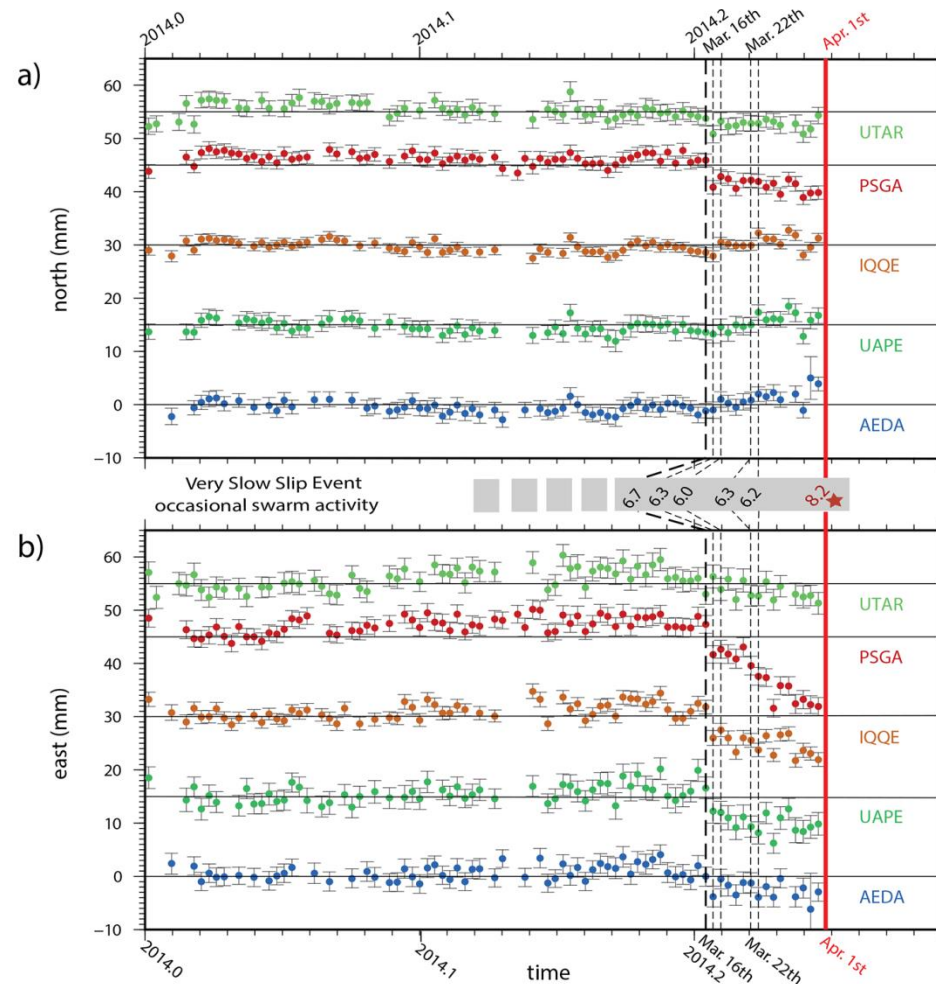


Fig. 3. Motion of coastal GPS stations preceding the Iquique earthquake. (A) North components and (B) East components relative to a linear evolution model with seasonal variations estimated since 2012 (14). The thick red line denotes the origin time of mainshock while the black dotted lines show the occurrence time of the $M_w > 6$ foreshocks.

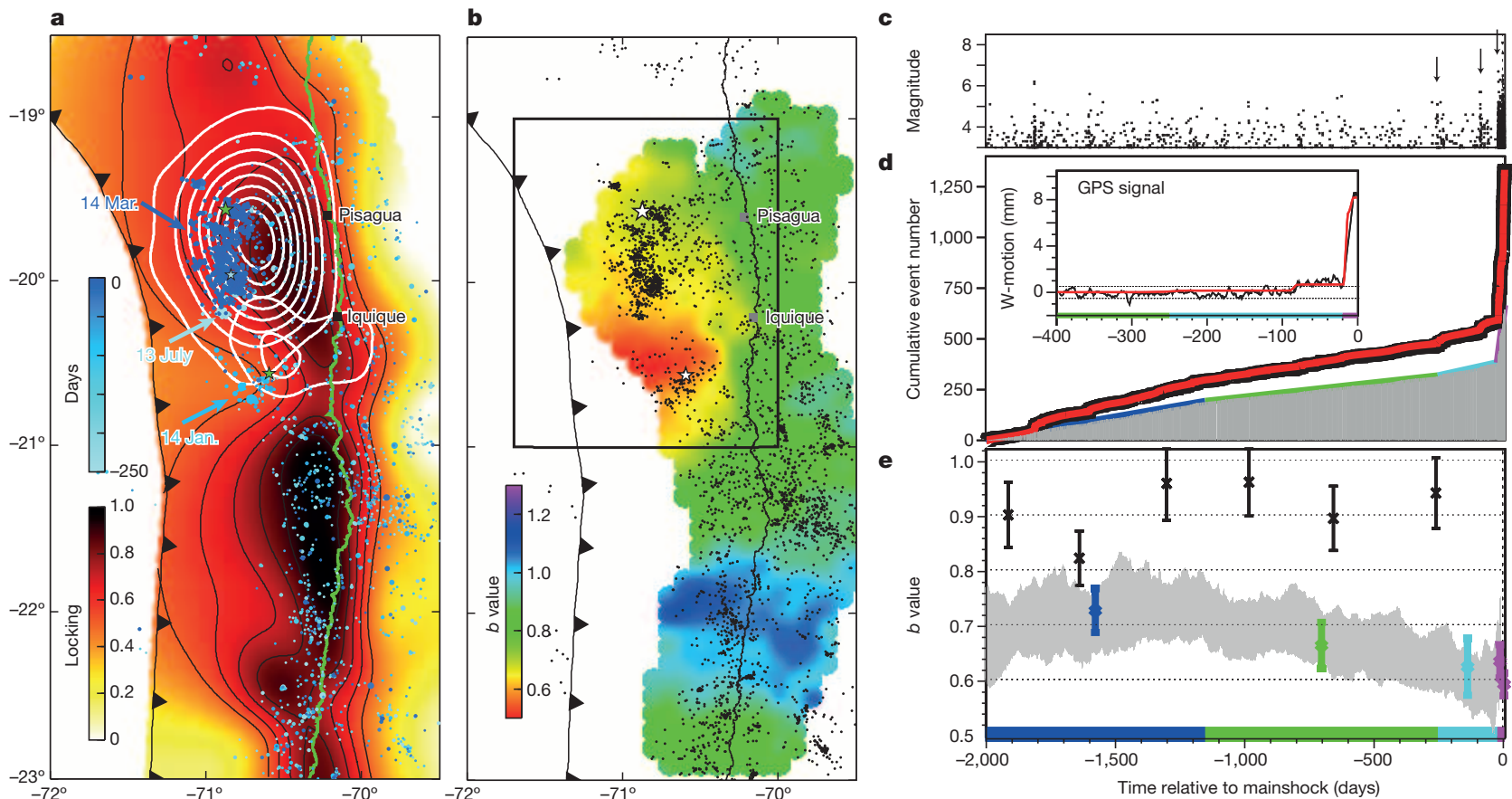


Figure 3 | Maps of interseismic locking and b value, and time history of seismicity and deformation. **a**, Geodetic interseismic locking and foreshocks. The July–August 2013, January and March 2014 foreshock clusters are marked. **b**, b -value map of the central portion of northern Chile gap for the last 2000 days before the mainshock, where results are calculated for all $M \geq 3$ foreshocks within 50 km if their number exceeds 100. The rectangular box encloses the area used for the results in **c–e**. **c**, Magnitude–time plot. Arrows mark the July–August 2013, January and March 2014 clusters. **d**, Observed (black thick line) and ETAS-modelled (red line) cumulative $M \geq 3$ activity; the thin coloured

lines are fits of the estimated background (grey shaded area) for the four phases, during each of which the background rate is almost constant (see the text). The inset shows measured GPS displacement time-series stacked from near-coast stations between 19° S and 21° S smoothed with a four-day moving average and the modelled signal related to cumulative slip of the foreshock events. **e**, Time series of b value (means \pm s.d.) for the events inside the box (coloured and grey shaded area). Black points and bars refer to the results for the events outside the box.

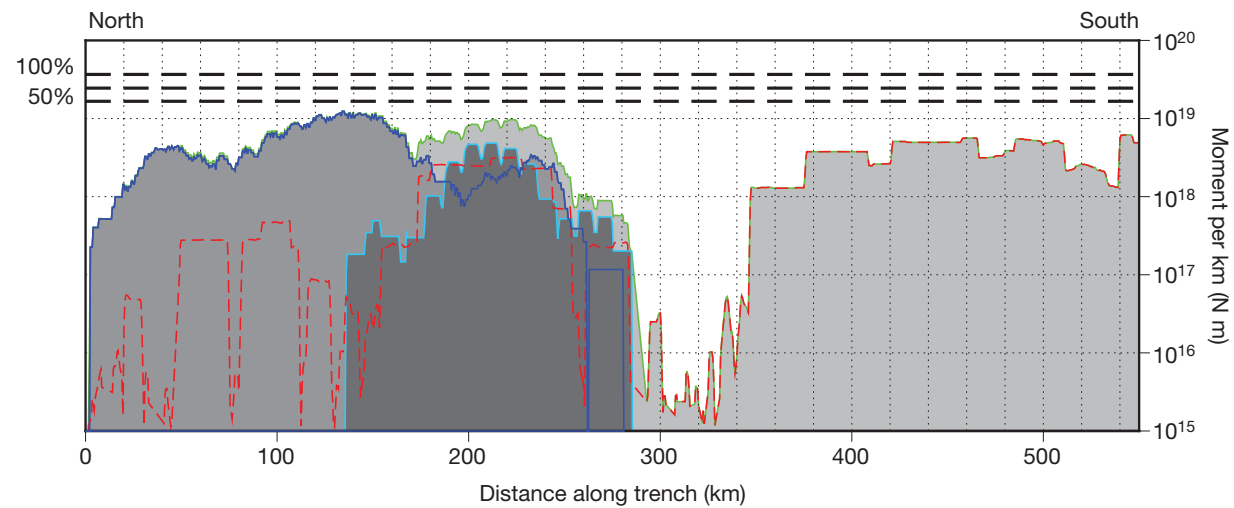


Figure 4 | Moment deficit along the northern Chile subduction zone. Moment calculated for historical seismicity from the USGS Combined Catalog³² since 1900, resolved as moment per kilometre along strike. For each earthquake, moment is divided evenly over the length of the rupture, calculated using empirical relations¹⁴. For the largest earthquakes ($M > 7.5$), more

accurate rupture areas are used⁸. Red shows moment for historical earthquakes; blue for 2014 seismicity (dark blue up to 3 April 2014; light blue since then); green represents all summed moment. Horizontal dashed lines represent moment accumulation levels given constant coupling percentages of 50%, 75% and 100%.

Referências

LETTER

doi:10.1038/nature13681

Gradual unlocking of plate boundary controlled initiation of the 2014 Iquique earthquake

Bernd Schurr¹, Günter Asch¹, Sebastian Hainzl¹, Jonathan Bedford¹, Andreas Hoechner¹, Mauro Palo¹, Rongjiang Wang¹, Marcos Moreno¹, Mitja Bartsch¹, Yong Zhang², Onno Oncken¹, Frederik Tilmann¹, Torsten Dahm¹, Pia Victor¹, Sergio Barrientos³ & Jean-Pierre Vilotte⁴

Geophysical Research Letters

RESEARCH LETTER

10.1002/2014GL060274

Key Points:
• 2014 Iquique earthquake rupture process inverted applying

Rupture process of the 2014 Iquique Chile Earthquake in relation with the foreshock activity

Yuji Yagi¹, Ryo Okuwaki², Bogdan Enescu¹, Shiro Hirano³, Yuta Yamagami², Suguru Endo², and Takuya Komoro²

Geophysical Research Letters

RESEARCH LETTER

10.1002/2014GL060238

Key Points:

• The 1 April 2014 Mw 8.1 earthquake

The 1 April 2014 Iquique, Chile, M_w 8.1 earthquake rupture sequence

Thorne Lay¹, Han Yue¹, Emily E. Brodsky¹, and Chao An²

GEOPHYSICS

Recognizing Foreshocks from the 1 April 2014 Chile Earthquake

Emily E. Brodsky and Thorne Lay

LETTER

doi:10.1038/nature13677

Continuing megathrust earthquake potential in Chile after the 2014 Iquique earthquake

Gavin P. Hayes¹, Matthew W. Herman², William D. Barnhart¹, Kevin P. Furlong², Sebastián Riquelme³, Harley M. Benz¹, Eric Bergman⁴, Sergio Barrientos³, Paul S. Earle¹ & Sergey Samsonov⁵

Geophysical Research Letters

RESEARCH LETTER

10.1002/2014GL061138

Key Points:

- Foreshocks migrated both along strike and down dip at rates of 2–10 km/d
- Slow-slip events occurred updip of the largest slip patch of the main shock rupture
- Final slow-slip event migrated to the initiation point of the main shock rupture

Multiple slow-slip events during a foreshock sequence of the 2014 Iquique, Chile M_w 8.1 earthquake

Aitaro Kato^{1,2} and Shigeki Nakagawa²

¹Earthquake and Volcano Research Center, Graduate School of Environmental Studies, Nagoya University, Nagoya, Japan,

²Earthquake Research Institute, University of Tokyo, Tokyo, Japan

Scienceexpress

Intense foreshocks and a slow slip event preceded the 2014 Iquique M_w 8.1 earthquake

S. Ruiz,^{1*} M. Metois,² A. Fuenzalida,³ J. Ruiz,¹ F. Leyton,⁴ R. Grandin,⁵ C. Vigny,⁶ R. Madariaga,⁶ J. Campos¹

